Improved Superconductive Mixer Coupling:
Sub-millimeter Performance without Sub-micron Lithography

J. A. Carpenter, E. R. Arambula, E. B. Guillory, A. D. Smith

TRW Space & Technology Group

Redondo Beach, CA 90278

Abstract

Superconductor-Insulator-Superconductor (SIS) mixers stand as the most sensitive heterodyne detectors of millimeter and sub-millimeter wave radiation. Nevertheless, scientists attempting to apply SIS mixers to sub-millimeter wavelengths have been forced to cope with limited dynamic range, critical tuning of junction capacitance, and difficult lithographic requirements.

This paper describes a novel RF-coupling scheme, in which an on-chip impedance transformer matches large, low impedance junctions to the high impedance of waveguide and free space. By operating low impedance junctions, the system dynamic range improves by 15 dB, while junction tuning become significantly easier.

A 100 GHz demonstration of the transformer-matched SIS mixer has been built, and shows wide bandwidth and large (35 dB) dynamic range. Used as a direct detector, the SIS junction shows full quantum-limited response and wide (8 GHz at 91 GHz center frequency) instantaneous detection bandwidth.

Introduction

Superconductive (SIS) mixers have proven to be ideally suited to radioastronomical applications from microwave to submillimeter wavelengths. The extreme nonlinearity of the superconductive tunnel junction current-voltage characteristics gives rise to high conversion efficiency, sometimes in excess of 0 dB, with added mixer noise approaching the quantum limit, $T_M = hf/k_B$. In

addition, these devices require mere nanowatts of local oscillator (LO) power, a key advantage in the LO-starved submillimeter environment.

Despite their advantages over semiconductor mixers, SIS mixers have two drawbacks over semiconductor mixers - limited saturation power and large capacitance. While the power limitation is not a severe constraint for radioastronomy, in which both signals and background noise levels are quite small, saturation power and associated dynamic range are key considerations several terrestrial applications including communications and imaging.

Limited saturation power is a direct result from the quantum mechanical nature of SIS mixers. SIS mixing is essentially a photon-assisted tunneling activity. When biased within a photon voltage (hf/e) below the junction gap voltage (Δ/e), conservation of energy dictates that absorption of a millimeterwave photon can induce an electron to tunnel across the junction barrier. The conversion of millimeterwave energy to junction current defines the mixing process. Optimum mixer gain requires that the operating voltage be held within a narrow range on a photon-assisted tunneling step. As a result, the SIS mixer is an output voltage-limited device. The resultant input saturation power, P_{sig}, for a single junction mixer is given by[1]:

$$P_{sig} \le (0.1 \text{ hf/e})^2/GR_{Dyn}, \qquad (1)$$

where G is the mixer conversion efficiency, R_{Dyn} is the loaded output resistance of the mixer, f is the frequency, and h and e are the conventional physical constants. Experiments at Berkeley confirmed this theoretical prediction, with measured saturation of only 1.5 pW for a 36 GHz mixer with gain. Thus saturation power limits single junction SIS mixers to narrowband, small signal detection with quiet backgrounds.

At the same time that single junctions were first being developed, series arrays of junctions were being used both to increase the saturation power and also to ease lithographic requirements in mixer fabrication. By going to a series array of N identical junctions[2], the saturation power of the SIS mixer increases to[3]

$$P_{sig} \leq N^2 \, (0.1 \, hf/e)^2 / GR_{Dyn}. \qquad (2)$$

This approach is illustrated in Table 1, line 1. In scaling the array, the total junction impedance is held fixed, and the individual junction resistances and areas are adjusted accordingly. Junction current density is held fixed.

Scaling to large arrays (with large saturation power) is complicated by junction capacitance. The relatively large capacitance of SIS junctions requires special care to efficiently couple power to the mixer elements. Researchers have attempted increasingly sophisticated technical approaches to avoid mixer saturation while maintaining the RF match necessary for maximum mixer sensitivity. Originally, mixer designs included single[4,5] or series-array[6] tunnel junctions(See Table 1, line 1.) These designs relied on external waveguide mechanical tuning elements, such as backshorts and tuning stubs, to inductively compensate for junction capacitance and other parasitic susceptances. This approach has achieved large gain and low noise, but only over a highly restricted bandwidth.

By adding an integrated tuning element, researchers were able to extend the instantaneous bandwidth while maintaining the gain and noise requirement necessary for sensitive mixing[7,8]. Table 1, line 2 diagrams this approach, with an array of junctions shown shunted by an on-chip tuning element such as an inductive stub. For millimeter wavelengths, the aggregate tuning approach limits the number of junctions in the array. Parasitic inductance along the series array of junctions, along the the capacitance of the individual junctions, gives rise to a LC resonance which prevents matching the waveguide signals.

Recently, workers have circumvented the LC resonance limitation by including a separate tuning structure at each mixer junction. This approach, shown in Table 1, line 3, can work up to much higher frequencies and much larger N than the other approaches. One difficulty in the separately tuned approach involves design tolerances. In order for the series bias current to produce identical operating voltage on each of the junctions, both the unpumped current-voltage characteristics and the rf embedding impedance must be identical for each of the junctions. The matching tolerance is

quite tight, especially for high gàin mixers, which have large dynamic resistance at the mixer operating point.

A fourth coupling scheme has been proposed and demonstrated using parallel and series array feeds. By using RF pass and RF block components, the current paths for IF and RF radiation can be completely separated. The approach of Ermakov, et al. [9],

In this paper, we propose and report results from a different type of SIS array. We overcome both fabrication and electrical difficulties by integrating an RF-matching transformer directly on the SIS chip.
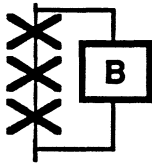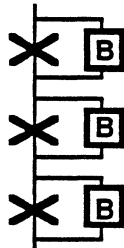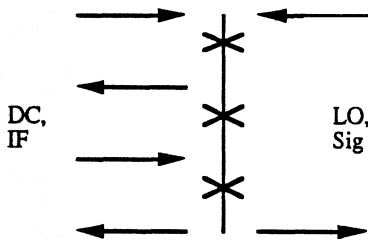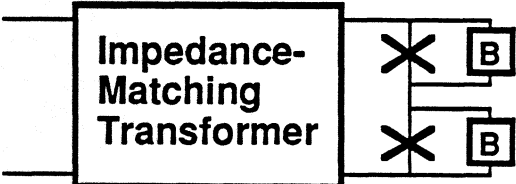
	Circuit schematic	Circuit description
1		Single or array of mixers with no integrated tuning element
2		Series array with aggregate tuning element
3		Series array with dedicated, integrated tuning
4		Rf series, IF parallel
5		2-element tuned array with impedance matching transformer

Table 1. SIS mixer chip architectures

Mixer Chip Design

Our mixer design procedure began with the selection of a mounting fixture. Raisenen, et al., have thoroughly modeled[10] and tested a waveguide mount for millimeter wave mixing. The mixer elements sits in the E-field orientation across a full-height waveguide. A mechanically adjustable backshort provides for broadband impedance matching.
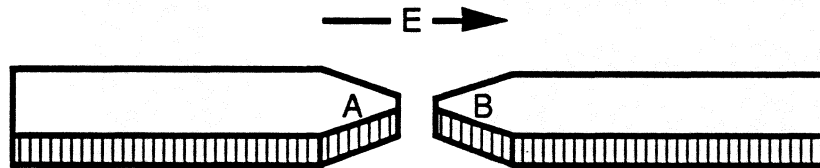
Figure 2. Electrode geometry. The E-field direction of the waveguide is shown.

The mixer element design must approximately match the impedance presented by the mixer block. Based upon the model measurements[9] a mixer element placed near the center of the waveguide and attached to RF-choked leads sees an embedding impedance of 60-100 Ω. Figure 2 shows the lead structure near the center of the waveguide. We maintained symmetry in our design, mirroring circuit patterns about the bisection plane.
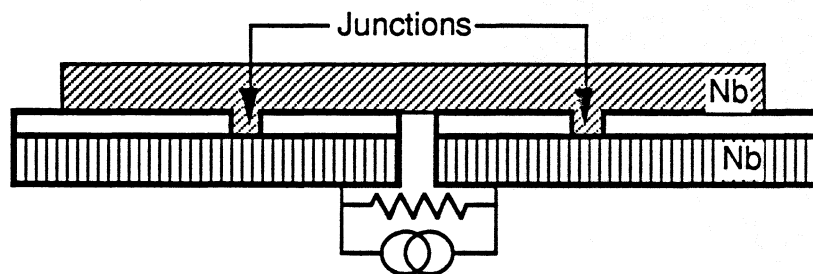
Figure 3. Mixer chip cross-sectional view. The lower niobium corresponds to the electrodes in Fig. 2. Dielectric layers are shown in white. Waveguide signals appear as the illustrated Norton equivalent across the electrodes.

We designed a microstrip transmission line transformer[11] to lower the source impedance seen by the mixer elements. The quarter wavelength transmission line extends from the electrode edge to the mixer junction, using the choke structure metallization as a groundplane. (See Fig. 3.) Each 8 Ω transmission line transforms the 30-50 Ω half-source impedance down to 1-2 Ω at the SIS tunnel junction.

A separate stub was added to tune out junction capacitance at the signal frequency. A series combination of high impedance line and quarter wavelength, open-ended low impedance line acted as a broadband, dc-blocking inductive element.
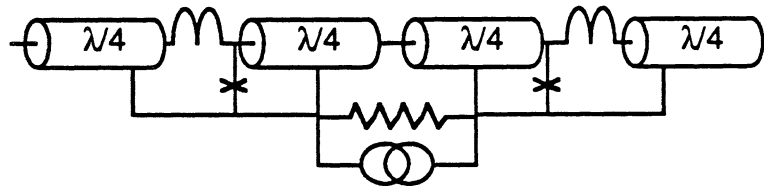

Figure 4. Electrical schematic of mixer chip. The central $\lambda/4$ microstrip transmission lines act as impedance transformers. The outside, open-ended $\lambda/4$ microstrip act as RF shorts. The inductors act to tune out junction capacitance at the signal frequency.

The transformer and susceptive matching network were implemented using the scheme shown in Fig. 4. All components, with the exception of the source and the junctions themselves, consisted of superconducting microstrip. The impedances of the microstrip were chosen to maximize mixer bandwidth. The quarterwave stubs were chosen as low impedance line, with short, high inductive microstrip directly connnecting to the junctions. We chose the impedance of the quarterwave transformers coupling the junctions to the antenna vertex to have impedances near the geometrical mean of the junction impedance and the antenna impedance.

The electric field distribribution is shown in Fig. 5. The tapered probe structure serves to concentrate the waveguide electric fields near the vertex. The vertex also serves as the launching point for microstrip modes propagating toward the tunnel junctions. Because the microstrip impedance is lower than the source impedance, standing waves form in the microstrip. Electric

fields tend to be highest near the vertex, while currents are large near the junctions.
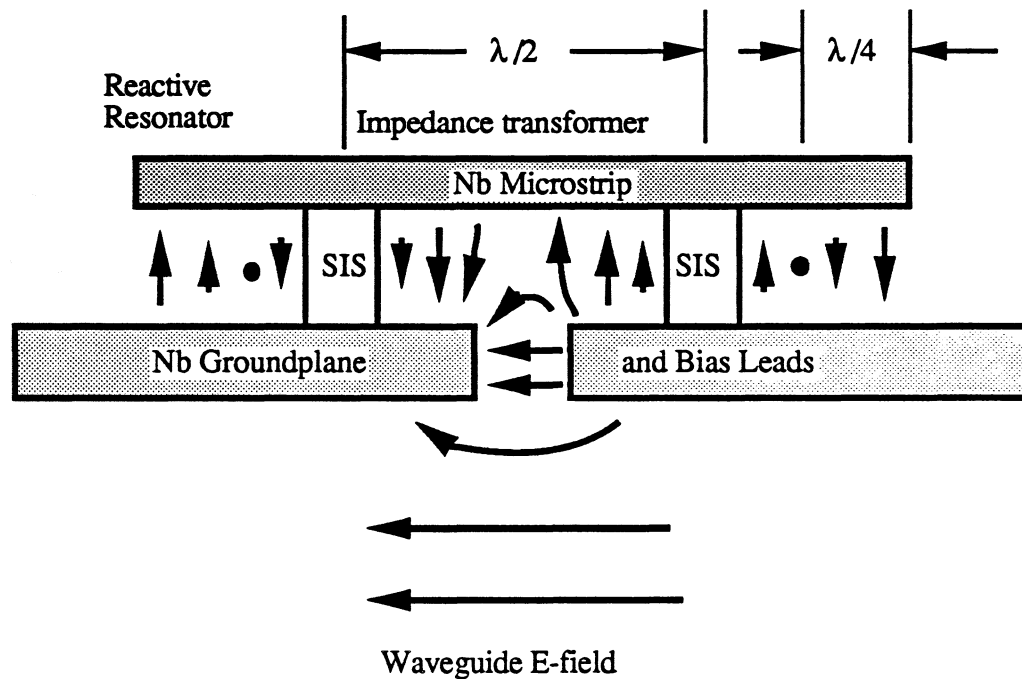
Figure 5. Electric fields for millimeterwave radiation. The vertex represents a high impedance point for the circuit, while the junction location is chosen as relatively low impedance.

Fabrication

The SIS mixers were prepared by depositing a trilayer structure of Nb/Al-AlO$_x$/Nb, onto a 5-mil quartz substrate. The base electrode of the trilayer (2000 Å), an aluminum layer, and the counter electrode (350 Å) were sputtered sequentially in a single vacuum chamber in an *in situ* process.[12] Immediately after the aluminum deposition, the samples were exposed to oxygen in a side-chamber of the deposition system in order to form the oxide tunneling barrier.

We fabricated the mixers using a 4-mask process. The junctions were defined by the selective niobium anodization process (SNAP)[13] with junction areas of 50 to 150 μm^2. These junction areas were considerably larger than the 1 - 10 μm^2 junction areas typical of SIS mixers. Isolation of each junction was achieved through a trilayer etch. In order to maintain tight tolerance of the etch process, a hybrid etch was developed. The Nb counter electrode was removed by RIE with

CF4 + 4% O2 plasma; the thin Al-AlOx layer was removed using a selective wet chemical etch. Finally, the Nb base electrode was removed again by RIE with the same plasma as the counter electrode. We patterned a layer of SiO on top of the junctions with a liftoff process. This mask allows a contact window for the final wiring. The wiring layer for the series connection of junctions and tuning structures was defined by a final RIE step.

SIS conversion efficiency and mixer noise depend strongly on the sub-gap leakage and abruptness of the current rise at $2\Delta/e$. The aluminum-based tunneling barrier plays a crucial role in determining the current-voltage characteristics of the SIS junctions. We therefore studied the aluminum thickness with the objective of optimizing junction characteristics essential for mixing.

In a series of experiments, we created a series of $Nb/Al-AlO_x/Nb$ trilayers with aluminum thicknesses varying from 30 to 200 Å. A constant aluminum sputtering rate of 1 Å/sec was maintained with varying deposition times to achieve the range of aluminum thicknesses. We found the optimum aluminum layer thickness to be 50 Å. Thinner aluminum barriers produce leakier junctions. Thicker aluminum barriers reduced the abruptness of the $2\Delta/e$ current rise.

We also found good thermal contact to a thermal sink is essential. Trilayers with good thermal contact to the cooled wafer substrate holder displayed distinctly sharper current-voltage characteristics than those with poor contact. Device yield was improved through the use of heat sink paper, which minimizes substrate heating during deposition.

Results

The mixer chips were mounted in the E-field direction of the full-height waveguide mount. No special electrostatic handling requirements were needed to perform the experiment, and no junction burn-outs were observed during testing. We attribute this reliability to the ruggedness of niobium junctions and the large junction areas (>50 square microns) made possible by the transformer

approach. We observed 3 dB responsivity bandwidths up to 8 GHz. These rf bandwidths are

within a factor of 2 of the fundamental bandwidth limit imposed by junction capacitance.

Our test procedure began with direct detection measurements. This allowed us to optimize the

backshort position for best signal coupling and also to measure the rf bandwidth. The quantum

limit for responsivity at 94 GHz is 2000 A/W if each photon enables one electron to flow across a

junction. If two junction transits are required for current flow, as is the case in our N=2 geometry,

the quantum limit reduces to 1000 A/W. The measured responsivities (see Fig. 5) were within

experimental uncertainty of the latter quantum limit. The high responsivities observed indicate a

good impedance match of the mixer circuit to the wave guide mount.
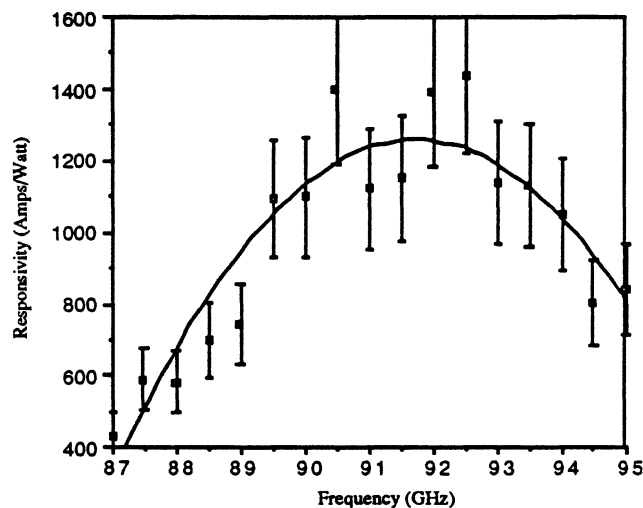

Figure 5. The measured responsivities of the mixer indicates good matching between the

waveguide and the mixer.

When operated as a mixer, our devices showed excellent performance. We observed negative resistance which indicates infinite *available* gain. Actual coupled gain (power delivered to the IF amplifier normalized to signal input power at the mixer block) was measured to +13 $\pm$1 dB. Useful mixing over 0.7 GHz was observed. Plotted in Figure 6 is the LO response showing a mixer with +10 dB gain. We attribute the wide swings in conversion efficiency to reflections and standing waves in the cable leading from our mixer to our room temperature IF amplifier. Current test apparatus limitations have prevented us from making accurate receiver noise temperature measurements.

The mixer instantaneous bandwidth is significantly narrower than the corresponding direct detector bandwidth. The reason appears simply related to the basic operation of the SIS mixer. While the direct detector bandwidth is limited by an $R_{rf}C$ time, the mixer bandwidth is additionally limited by a IF bandwidth time constant of $R_{dc}C$. Since the dynamic resistance, R_{dc}, of the pumped junction is always significantly larger than the RF junction impedance, a stricter bandwidth limit will always appear for SIS junctions. This observation is consistent with our data.
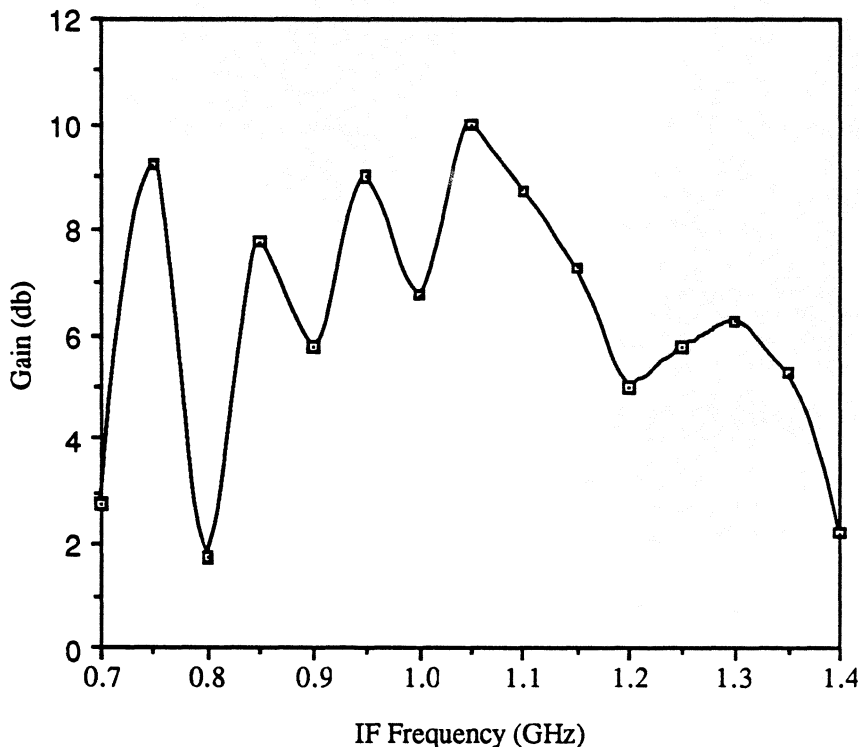
Figure 6. IF response showing mixer gain.

The power handling capacity of the transformer mixer is shown in Fig. 7. The particular mixer demonstrates over 30 dB of linear response, limited by our measurement capabilities. As shown the mixer is of low gain operating with -4 dB conversion efficiency. Nevertheless the enhancement in output power over conventional SIS mixers is apparent. Whereas conventional single junction 94 GHz mixers tend to saturate at -75 dBm output levels, our mixer delivered -55 dBm with no appreciable nonlinearity. Of the 20 dB power enhancement, we attribute 6 dB to the N=2 geometry, and 14 dB to impedance reduction.
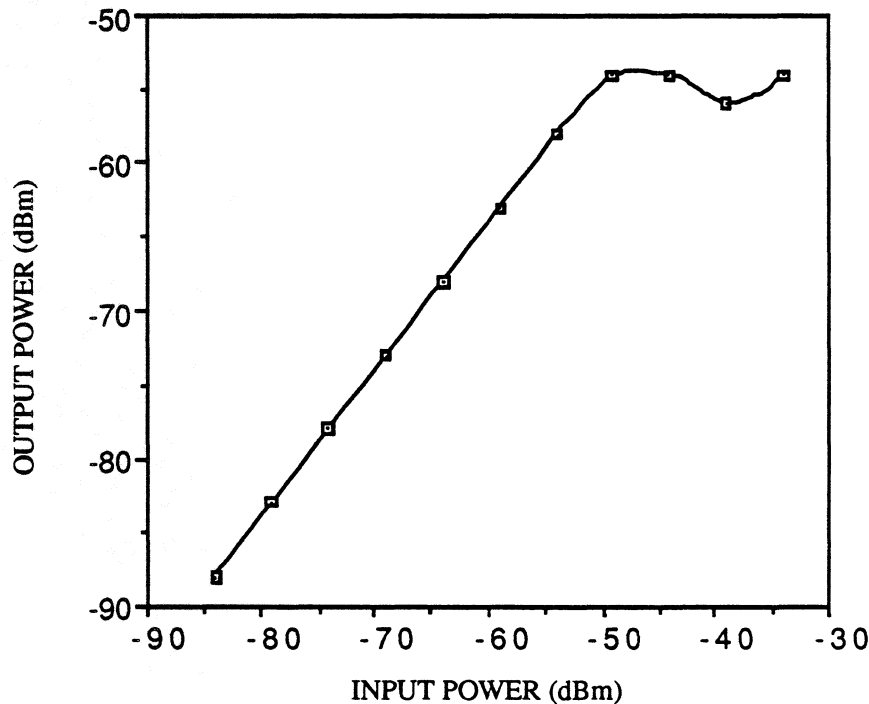

Figure 7. Saturation power of mixer with conversion gain.

Conclusions

We have developed a new type of SIS waveguide mixer circuit, using an integrated input transformer. The new circuit enhances the saturation power of the SIS mixer by 20 dB over conventional radiotelescopic single junction mixers. A simple quarterwave transmission line

provides good rf match over wide bandwidths. In addition, the SIS mixer's large junction design reduces device burn-out and eases fabrication. The 20 dB increase in saturation power will allow the application of the mixer to communication and radar systems.

Acknowledgements

References

1 A. D. Smith and P. L. Richards, "Analytic Solutions to Superconductor-Insulator-Superconductor Quantum Mixer Theory," J. Appl. Phys. 53, 3806-3812, 1982.

2 S. Rudner and T. Claeson, Appl. Phys. Lett. 34, 711 (1979).

3 S. Rudner and T. Claeson, Appl. Phys. Lett. 34, 711 (1979).

4 G. J. Dolan, T. G. Phillips, D. P. Woody, "Low-noise 115–GHz mixing in superconducting oxide-barrier tunnel junctions", Appl. Phys. Lett. 34, 347-349 (1979).

5 W. R. McGrath, P. L. Richards, A. D. Smith, H. van Kempen, R. A Batchelor, D. E. Prober, and P. Santhanam, Appl. Phys. Lett. 39, 655-658 (1981).

6 S. Rudner, M. J. Feldman, E. Kollberg, and T. Claeson, IEEE Trans. Magn. MAG-17, 690-693 (1981).

7 Q. Hu, C. A. Mears, P. L. Richards, and F. L. Lloyd, "Measurement of integrated tuning elements for SIS mixers with a Fourier transform spectrometer", Int. J. Infrared Millim. Waves 9, 303-320 (1988).

8 S.-K. Pan, A. R. Kerr, M. J. Feldman, A. W. Kleinsasser, J. Stasiak, R. L. Sandstrom, and W. J. Gallagher, "An SIS mixer for 85-116 GHz using inductively shunted edge-junctions",1988 IEEE MTT International Microwave Symposium Digest, 465-468 (1988).

9 An. B. Ermakov, V. P. Koshelets, S. A. Kovtonyuk, and S. V. Shitov, "Parallel Biased SIS-Arrays for MM Wave Mixers, to be published in ASC '90 proceedings.

10 A.V. Raisanen, W.R. McGrath, D.G. Crete, P.L. Richards, "Scaled Model Measurements of Embedding Impedances for SIS Waveguide Mixers", International Journal of Infrared and Millimeter Waves, Vol.6, No.12,1169-1189,1985.

11 V. Yu. Belitsky, I. L. Serpuchenko, M. A. Tarasov, and A. N. Vystavkin, "MM Waves Detection Using Integrated Structure with SIS Junction, Stripline Transformer and Spiral Antenna", Extended Abstracts of 1989 International Superconductivity Electronics Conference (ISEC '89), 179-182, (1989).

12 J. M. Murduck, J. Porter, W. Dozier, R. Sandell, J. Burch, J. Bulman, C. Dang, L. Lee, H. Chan, R. W. Simon, and A. H. Silver, "Niobium trilayer Process for Superconducting Circuits", IEEE Trans. Magn. MAG-25, 1139-1142, (1989).

13 H. Kroger, L. N. Smith, D. W. Jillie, "Selective Niobium Anodization Process for Fabricating Josephson Tunnel Junctions,", Appl. Phys. Lett. 39, 280-282, 1981.